



# The Effects of Mechanical Stretch on Integrins and Filopodial-Associated Proteins in Normal and Glaucomatous Trabecular Meshwork Cells

Yong-Feng Yang<sup>1</sup>, Ying Ying Sun<sup>1</sup>, Donna M. Peters<sup>2</sup> and Kate E. Keller<sup>1,3\*</sup>

<sup>1</sup>Casey Eye Institute, Oregon Health & Science University, Portland, OR, United States, <sup>2</sup>Department of Pathology and Laboratory Medicine, University of Wisconsin School of Medicine and Public Health, Madison, WI, United States, <sup>3</sup>Department of Chemical Physiology and Biochemistry, Oregon Health & Science University, Portland, OR, United States

## OPEN ACCESS

### Edited by:

Claudia Tanja Mierke,  
Leipzig University, Germany

### Reviewed by:

Padmanabhan Paranjii Pattabiraman,  
Purdue University Indianapolis,  
United States  
Abbot Clark,  
University of North Texas Health  
Science Center, United States

### \*Correspondence:

Kate E. Keller  
gregorka@ohsu.edu

### Specialty section:

This article was submitted to  
Cell Adhesion and Migration,  
a section of the journal  
Frontiers in Cell and Developmental  
Biology

Received: 28 February 2022

Accepted: 11 April 2022

Published: 29 April 2022

### Citation:

Yang Y-F, Sun YY, Peters DM and  
Keller KE (2022) The Effects of  
Mechanical Stretch on Integrins and  
Filopodial-Associated Proteins in  
Normal and Glaucomatous Trabecular  
Meshwork Cells.  
Front. Cell Dev. Biol. 10:886706.  
doi: 10.3389/fcell.2022.886706

The trabecular meshwork (TM) is the tissue responsible for regulating aqueous humor fluid egress from the anterior eye. If drainage is impaired, intraocular pressure (IOP) becomes elevated, which is a primary risk factor for primary open angle glaucoma. TM cells sense elevated IOP via changes in their biomechanical environment. Filopodia cellular protrusions and integrin transmembrane proteins may play roles in detecting IOP elevation, yet this has not been studied in detail in the TM. Here, we investigate integrins and filopodial proteins, such as myosin-X (Myo10), in response to mechanical stretch, an *in vitro* technique that produces mechanical alterations mimicking elevated IOP. Pull-down assays showed Myo10 binding to  $\alpha 5$  but not the  $\beta 1$  subunit,  $\alpha \nu \beta 3$ , and  $\alpha \nu \beta 5$  integrins. Several of these integrins colocalized in nascent adhesions in the filopodial tip and shaft. Using conformation-specific antibodies, we found that  $\beta 1$  integrin, but not  $\alpha 5$  or  $\alpha \nu \beta 3$  integrins, were activated following 1-h mechanical stretch. Cadherin -11 (CDH11), a cell adhesion molecule, did not bind to Myo10, but was associated with filopodia. Interestingly, CDH11 was downregulated on the TM cell surface following 1-h mechanical stretch. In glaucoma cells, CDH11 protein levels were increased. Finally, mechanical stretch caused a small, yet significant increase in Myo10 protein levels in glaucoma cells, but did not affect cellular communication of fluorescent vesicles via filopodia-like tunneling nanotubes. Together, these data suggest that TM cell adhesion proteins,  $\beta 1$  integrin and CDH11, have relatively rapid responses to mechanical stretch, which suggests a central role in sensing changes in IOP elevation *in situ*.

**Keywords:** glaucoma, trabecular meshwork, filopodia, integrins, tunneling nanotubes, myosin-X, cadherin-11, mechanosensing

## INTRODUCTION

Glaucoma is a leading cause of blindness, with a global prevalence of 3.54% in the population aged 40–80 years (Tham et al., 2014). A major risk factor of glaucoma is elevated intraocular pressure (IOP), which is caused by dysfunction in the trabecular meshwork (TM) aqueous humor drainage pathway (Stamer and Acott, 2012). The extracellular matrix (ECM) of TM tissue is a source of outflow resistance and glaucomatous ECM differs in amount, structure and organization compared to normal TM tissue (Fuchshofer and Tamm, 2009; Tektas and Lutjen-Drecoll, 2009; Vranka et al.,

2015; Acott et al., 2021; Keller and Peters, 2022). Glaucomatous TM tissue has altered biomechanics compared to age-matched tissue derived from non-glaucomatous TM tissue (Last et al., 2011; Raghunathan et al., 2018). Notably, glaucoma TM cells in culture display molecular memory and synthesize and assemble dysfunctional matrices similar to those found *in situ* (Raghunathan et al., 2018; Acott et al., 2021; Wirtz et al., 2021). During a normal homeostatic response to elevated IOP, stretch and/or distortion of transmembrane mechanosensors activate downstream signaling pathways, which ultimately adjust aqueous outflow (Acott et al., 2021). Integrins have been implicated in the detection of elevated IOP (Gagen et al., 2014; Filla et al., 2017; Faralli et al., 2019). Their extracellular domains bind ECM molecules such as fibronectin and collagens, thus sensing alterations in extracellular biomechanical cues caused by elevated IOP. Integrins then switch from a bent, inactive conformation to an active state (Filla et al., 2017). Mechanical forces activate  $\alpha 5 \beta 1$ , or  $\alpha v \beta 3$  integrins, in fibroblasts and endothelial cells, respectively (Tzima et al., 2001; Katsumi et al., 2005). Yet, this has not been studied in TM cells. A tightly coordinated regime of cellular mechanosensing, mechanotransduction, and ECM remodeling is required to precisely coordinate homeostatic responses to elevated IOP.

Filopodia are projections that extend from the cell surface and are important for mechanosensing, phagocytosis, and fundamental cellular processes such as cell adhesion, migration, spreading, division and growth factor signaling (Mattila and Lappalainen, 2008). Using live cell imaging, we previously showed that highly dynamic filopodia emanate from TM cells and these can extend over long distances ( $> 100 \mu\text{m}$ ) in cells and tissue (Keller et al., 2017; Sun et al., 2019a; Keller and Kopczynski, 2020). Filopodia growth involves multiple steps and various proteins are found at the base, the shaft, or at the tip of the filopodia (Mattila and Lappalainen, 2008). The identity and location of filopodial proteins is cell-type dependent (Ljubojevic et al., 2021). Filopodial base proteins include Arp2/3, filopodial shaft proteins include  $\beta 1$  integrins, epidermal growth factor receptor pathway 8 (Eps8), and fascin, while proteins found at filopodial tips include myosin-X (Myo10), mDia2 (also known as Diaph3), and  $\beta 1$ -integrin (Mattila and Lappalainen, 2008; Watanabe et al., 2010). Interestingly, in U2OS cells, Myo10 binds to  $\alpha 5 \beta 1$  integrin, where it functions to transport these integrin subunits toward to the filopodial tip (Miihkinen et al., 2021). Several cadherins are also involved in filopodia formation and extension in endothelial and neuronal cells, as well as in mouse embryos (Almagro et al., 2010; Fierro-Gonzalez et al., 2013; Lai et al., 2015). Cadherin-11 (CDH11), also known as OB-cadherin, plays a role in cell-cell adhesion and cell-ECM adhesion (Langhe et al., 2016), and it has strong expression in TM cells where it is up-regulated by TGF $\beta 2$  (Wecker et al., 2013; Webber et al., 2018). However, CDH11 has not been investigated regarding filopodia in TM cells.

Tunneling nanotubes (TNTs) are filopodia-like structures that are important for cellular communication (Ljubojevic et al., 2021). Since their discovery in 2004, TNTs have been described in many cells types where they transport large

cellular organelles (lysosomes, mitochondria, endosomes) and smaller cargoes (viruses, microRNAs, signaling molecules) between neighboring cells through a tube connecting their cytoplasm (Rustom et al., 2004). We have described TNTs in normal TM cells as well as glaucoma TM cells (Keller et al., 2017; Sun et al., 2019a). Communication via TNTs is advantageous in the aqueous environment of the anterior eye since cargoes can be directly transported between cells and signals are not diluted in aqueous fluid. Moreover, TNTs can extend up to  $100 \mu\text{m}$  in tissue, which allows cells to communicate over long distances (Keller et al., 2017; Ljubojevic et al., 2021). This potentially allows cells located on separate TM beams to coordinated responses to elevated IOP *in situ*. Myo10 is a quintessential filopodial protein that is important for TNT formation (Berg and Cheney, 2002; Bohil et al., 2006; Watanabe et al., 2010; Gousset et al., 2013). Myo10 protein distribution is altered in glaucomatous TM tissue and Myo10 gene silencing reduces outflow through the TM (Sun et al., 2019a; Sun et al., 2019b). This implicates a role for Myo10 in IOP homeostasis.

Filopodia and integrins are mechanosensors likely involved in sensing changes to the TM biomechanical environment caused by elevated IOP. Therefore, we investigated the effects of mechanical stretch on filopodia-associated proteins, Myo10 protein interactions, and cellular communication via TNTs in normal and glaucomatous TM cells.

## METHODS

### Primary Trabecular Meshwork Cell Culture

Normal (NTM) and glaucoma (GTM) cells were cultured from TM tissue dissected from human cadaver eyes (Lions VisionGift, Portland, OR) using established techniques (Keller et al., 2018). Donor information was de-identified prior to use and use of cadaver eyes was considered exempt by OHSU Institutional Review Board. Demographics of human donor eyes are in **Supplementary Table S1**. All TM cells were used prior to passage six and were characterized by monitoring cell phenotype by phase microscopy, and by induction of myocilin protein by dexamethasone treatment (**Supplementary Figure S1**) (Keller et al., 2018). Characterization for some cell strains are already published (Sun et al., 2019a; Sun et al., 2019b).

### Co-Immunoprecipitation Assays

Myosin-10 polyclonal antibody was incubated overnight with protein A/G Magnetic Beads (Pierce). Following washing with phosphate buffered saline with 0.05% Tween (PBST) and blocking with bovine serum albumin, the Myo10-antibody beads were incubated with TM RIPA lysates with 10 mM MgCl $_2$  overnight at 4°C. The tubes were then placed in a magnetic holder so Myo10 antibody-coated magnetic beads remained in the tube while they were washed thoroughly with PBST. After the final wash, 1x SDS-PAGE sample buffer was added to the tube, samples were boiled, and immunoprecipitated proteins were separated by SDS-PAGE. Following transfer, nitrocellulose membranes were probed with either integrin  $\beta 1$ ,  $\alpha 5$ ,  $\alpha v \beta 3$ ,  $\alpha v \beta 5$ , or CDH11 primary antibodies (**Supplementary**

**Table S2).** Secondary antibodies were IRDye 700-conjugated anti-rabbit or IRDye 800-conjugated anti-mouse antibodies (Rockland). Membranes were scanned using an Odyssey gel imaging system (Licor, Lincoln, NE, United States).

## Mechanical Stretch

Mechanical stretch experiments were performed as described previously (Bradley et al., 2001). Briefly, TM cells were seeded on 6-well collagen type I-coated silicone membranes (FlexCell International, Burlington, NC) and grown to confluence. Cells were made serum-free and the membrane was stretched over a pushpin head for either 1 h (immunohistochemistry experiments) or 24 h (Western immunoblots). The upward inversion of the membrane with the cells attached produces a static radial and circumferential stretch of approximately 10% (Bradley et al., 2001). For comparison, an IOP of 30 mmHg was estimated to produce a mechanical stretch of outflow pathway cells of up to 50% *in situ* (Grierson and Lee, 1977).

## Immunohistochemistry and Confocal Microscopy

To investigate filopodial proteins, immunohistochemistry was performed. One hour prior to fixation, SiR-actin (Cytoskeleton, Inc.) and 10  $\mu$ M verapamil, which increases fluorescent signal of SiR-actin, was added to the cultures (Keller and Koczynski, 2020). Silicone membranes were removed from the plates and fixed with 4% paraformaldehyde. Following permeabilization in 0.03% Tween-20 and blocking with CAS-block (Invitrogen), primary antibodies (**Supplementary Table S2**) were incubated. After washing, Alex Fluor 488- or 594-conjugated species-specific secondary antibodies were incubated and coverslips were mounted on top of silicone membranes in DAPI-containing ProLong gold (Invitrogen). Fluorescence images were captured using an Olympus FV1000 confocal microscope using identical acquisition settings for each treatment (e.g., stretch vs. non-stretch). For CDH11 immunostaining, TM cells were graded as having high CDH11, medium, or low/no CDH11 based on fluorescence intensity. Grading was performed independently by two authors in a masked manner. To quantitatively assess integrin activation, Image J was used to measure total fluorescence in a field and the number of DAPI-stained nuclei was counted. Total activated integrin fluorescence was normalized for the number of nuclei, then data were averaged and a standard error calculated.

## Western Immunoblotting

RIPA lysates were harvested on ice from confluent NTM and GTM cells, or from TM cells that were mechanically stretched for 24 h. A 24 h time point was used so that changes in protein levels could accumulate. After harvesting, protease cocktail inhibitor was added to the RIPA lysates, proteins were separated by SDS-PAGE and Western immunoblots were performed with the indicated primary antibodies (**Supplementary Table S2**). Total ERK1 or tubulin

antibodies were used as a loading control. Secondary antibodies were IRDye 700-conjugated anti-rabbit or IRDye 800-conjugated anti-mouse antibodies. Membranes were scanned using an Odyssey gel imaging system. Bands were quantitated from each lane of the immunoblots using ImageJ software and relative fluorescent units (RFUs) data were normalized for loading. For comparing mechanical stretch, RFUs of mechanically stretched TM cells were made a percentage of non-stretched RFUs for each cell strain. Data were averaged and plotted on the graph.

## Tunneling Nanotubes Vesicle Transfer Assay

A vesicle transfer assay quantitated fluorescent vesicle transfer via TNTs between cells (Abounit et al., 2015; Keller et al., 2017; Sun et al., 2019a) Briefly, cells were labeled with 1  $\mu$ M of either Vybrant DiO (488 nm) or DiD (647 nm) dyes (ThermoFisher), mixed 1:1, and plated at  $1 \times 10^5$  cells/ml on FlexCell membranes. Cells were allowed to adhere for 2 h and then the membranes with attached cells were mechanically stretched for 24 h. Cells were fixed and immunostained with rat monoclonal anti-CD44, clone IM-7 (Stem Cell Technologies, Vancouver, BC) and Alexa-fluor 594-conjugated donkey anti-rat secondary antibody (ThermoFisher) to visualize the cell membrane. Confocal z-stacked images were acquired and the total number of DiO (green) and DiD (red)-labeled cells in each image were counted. The number of TM cells containing at least five vesicles of the opposite color (transferred vesicles) was then made a percentage of total cell number, as described previously (Keller et al., 2017; Sun et al., 2019a).

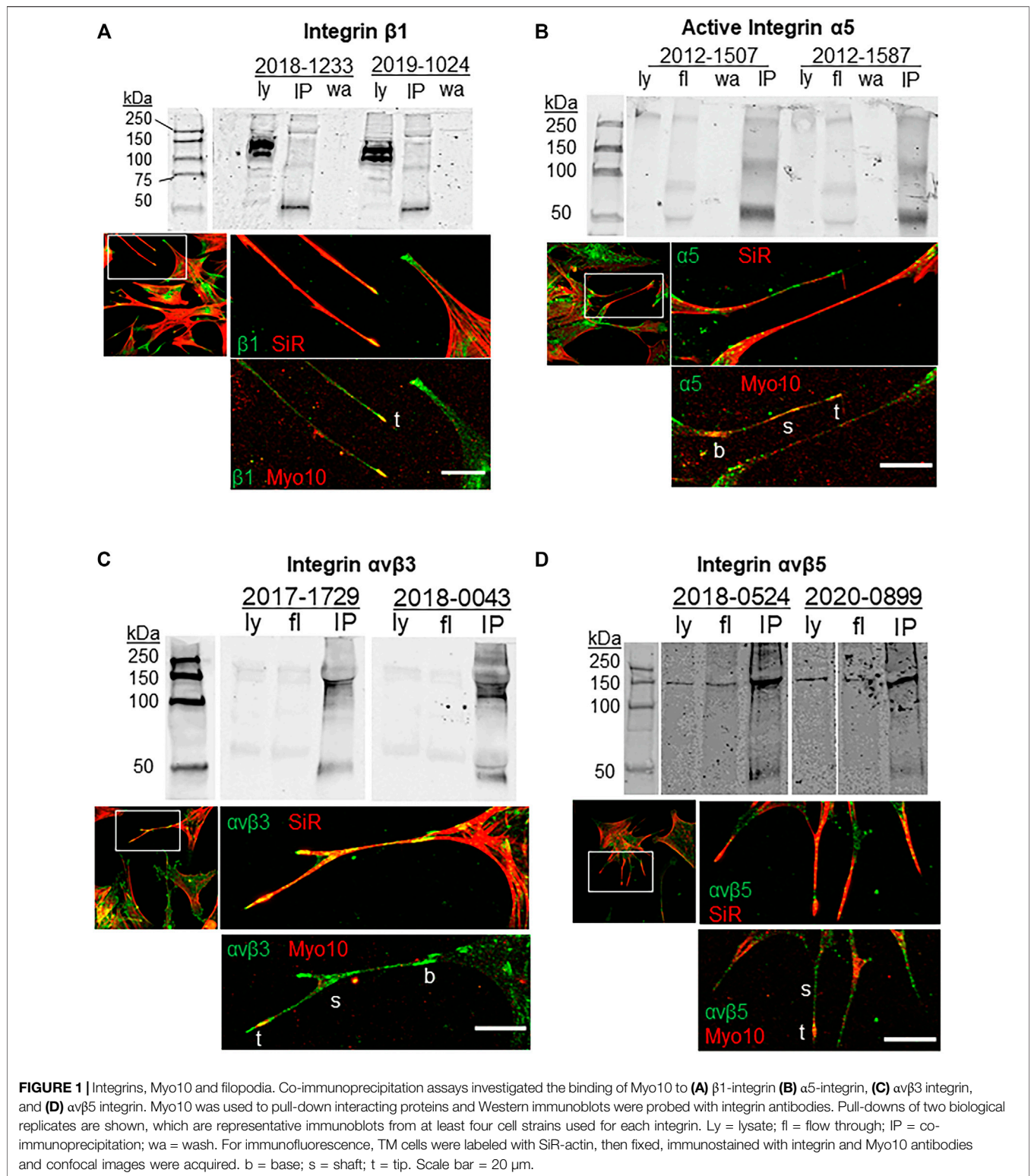
## Statistics

Biological ( $>n = 3$ ) and technical ( $>n = 3$ ) replicates were performed for all the experiments. The n's are reported in the figure legends. Data are reported as mean  $\pm$  standard error. One-way ANOVA with a post-hoc Tukey test, or a paired Students t-test, were performed. Significance was set at  $p < 0.05$ .

## RESULTS

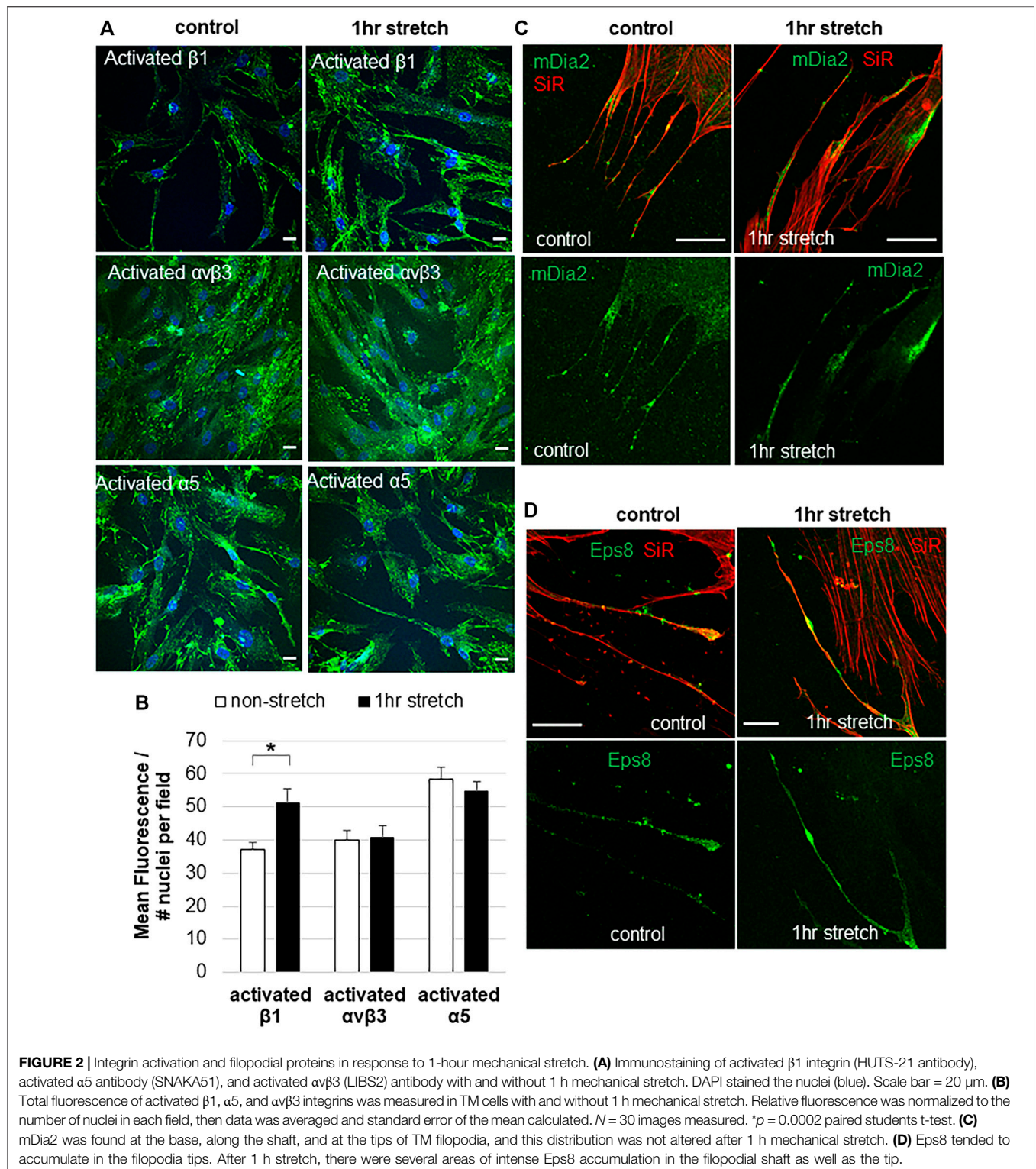
### Integrins and Myosin-X Interactions

Previous studies indicated that  $\beta 1$  integrins and  $\alpha 5$  integrins are transported along filopodia by Myo10 (Zhang et al., 2004; He et al., 2017; Miihkinen et al., 2021). Here, we investigated the co-localization of integrins with Myo10 in filopodia of TM cells and performed co-immunoprecipitation assays to examine Myo10-integrin protein interactions (**Figure 1**).  $\beta 1$  integrin strongly colocalized with Myo10 at the tips of filopodia, while along the shaft the  $\beta 1$  fluorescent signal was lower and there were only a few areas of colocalization (**Figure 1A**). Activated  $\alpha 5$  integrin showed colocalization with Myo10 along the shaft and at the filopodia tip (**Figure 1B**). The localization of  $\alpha v\beta 3$  and



$\alpha \beta 5$  integrins were also examined. There was a strong fluorescence signal for  $\alpha \beta 3$  integrin along the filopodial shaft and at the tip (Figure 1C), but the signal for  $\alpha \beta 5$

integrin showed much lower fluorescence (Figure 1D) suggesting that there were lower levels of  $\alpha \beta 5$  integrin in filopodia.



To determine if Myo10 and these integrins interacted, we performed pull-down assays using a Myo10 antibody. As shown in **Figure 1**,  $\alpha 5$  (116 kDa),  $\beta 3$  and  $\beta 5$  integrin subunits (~135 kDa) were pulled down using the Myo10 antibody, but we failed to show an interaction between Myo10 and the  $\beta 1$

integrin subunit (140 kDa). All pull-down lanes showed a band at ~50 kDa, which corresponds to the IgG heavy chain. Together, these data expand the repertoire of integrins that bind to Myo10, but lack of binding to the  $\beta 1$  integrin subunit suggests that Myo10- $\beta 1$  integrin interactions are cell-type dependent.

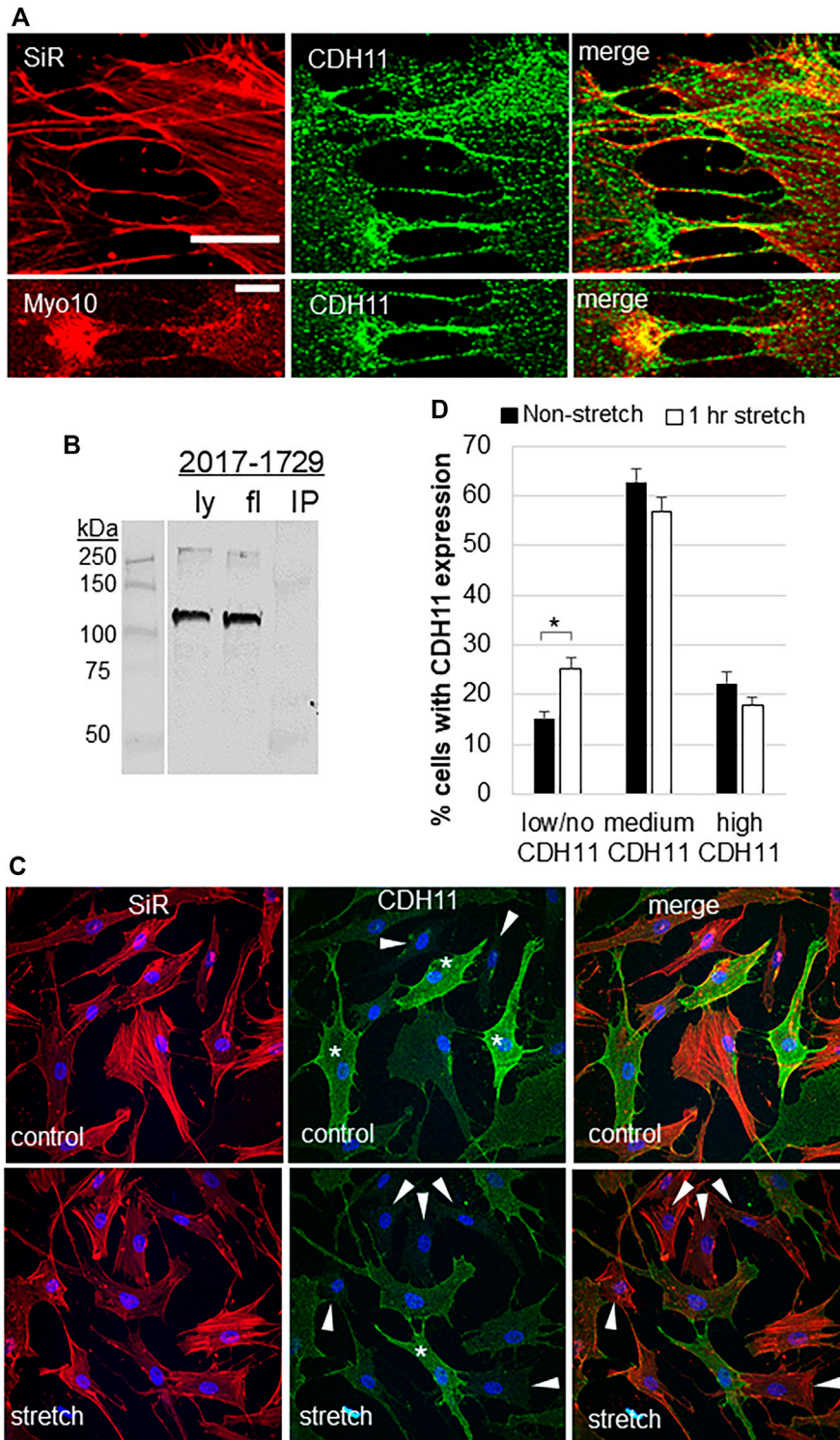


**FIGURE 3** | Cadherin-11 in filopodia and in response to mechanical stretch. **(A)** CDH11 was found along the length of filopodia or TNTs connecting adjacent TM cells. CDH11 colocalized with Myo10 at the base of the filopodia, but not along its length. Scale bar = 20  $\mu$ m. **(B)** CDH11 did not bind to Myo10 in pull-down assays. Ly = lysate; fl = flow-through; IP = immunoprecipitated proteins. **(C)** TM cells were mechanically stretched for 1-h then fixed and stained with CDH11 (green). Actin (red) and DAPI (blue) identified all the TM cells in a field. Cells with high (\*), medium, and low/no (arrowheads) CDH11 levels were identified. **(D)** High, medium, and low CDH11 cells were counted and made a percentage of the total number of cells. \* $p < 0.015$  by ANOVA. Data show mean  $\pm$  s.e.m.

## Trabecular Meshwork Filopodial Proteins in Response to Mechanical Stretch

Mechanical stretch is an *in vitro* method to mimic elevated IOP (Bradley et al., 2001). Integrins may play a central role in detecting changes in mechanical forces caused by elevated IOP (Acott and Kelley, 2008; Gagen et al., 2014; Filla et al., 2017; Acott et al., 2021), but this has not been directly tested. Here, we investigated the effects of a static mechanical stretch on integrin activation. A 1-h mechanical stretch was chosen because live cell imaging shows that mechanosensing filopodia protrude from the TM cell surface in this time frame (Keller et al., 2017; Keller and Koczynski, 2020). To detect activated integrins, we used HUTS-21, SNAKA51, and LIBS2 conformation-specific monoclonal antibodies, which detect activated forms of  $\beta 1$ ,  $\alpha 5$  and  $\alpha v \beta 3$  integrins, respectively (Du et al., 1993; Luque et al., 1996; Clark et al., 2005; Byron et al., 2009). There was significantly increased fluorescent signal for activated  $\beta 1$  integrin in TM cells following 1 h mechanical stretch (Figure 2A,B). This increase in activated  $\beta 1$  integrin represented the entire field and was not specifically localized to filopodia. However, there was no difference in the fluorescent signal of activated  $\alpha 5$ , or activated  $\alpha v \beta 3$ , in stretched vs. non-stretched TM cells. A conformation-specific antibody to activated  $\alpha v \beta 5$  is not available so we could not assess this subtype.

In addition to integrins, we investigated the distribution of filopodial proteins Eps8 and mDia2 in non-stretched vs. stretched TM cells. In non-stretched TM cells, mDia2 was localized to the base, shaft, and tip of filopodia (Figure 2C), while Eps8 was localized to discrete patches in the shaft and at the tips of filopodia (Figure 2D). mDia2 showed increased areas in the filopodia following mechanical stretch, suggestive of enhanced nascent adhesions.

## Cadherin-11 and Filopodia

CDH11 is a cell adhesion protein, which is highly expressed in TM cells (Webber et al., 2018). The filopodial protein Myo10 binds to other cadherin family members (Almagro et al., 2010; Lai et al., 2015). Therefore, we investigated CDH11 localization in TM cells. CDH11 localized as punctate dots at the TM cell surface and strongly decorated the base and the entire length of the filopodia (Figure 3A). CDH11 at the filopodial base colocalized with Myo10, but not in the shaft. However, pull-down assays failed to detect an interaction between Myo10 and CDH11 (Figure 3B). We also observed that CDH11 fluorescence was variable, where some TM cells showed high CDH11 levels, others had a medium level of CDH11, while others have little to no CDH11 immunostaining (Figure 3C). We counted the number of high, medium, and low CDH11 cells, with and without 1-h mechanical stretch. Interestingly, the number of low CDH11-expressing cells was significantly higher in stretched than non-stretched cells (Figure 3D) suggesting that mechanical stretch decreased the number of CDH11-positive TM cells.

## Effect of Mechanical Stretch in Normal and Glaucomatous Trabecular Meshwork Cells

CDH11 is up-regulated in diseases associated with excess ECM deposition such as invasive breast cancer, scleroderma, and liver fibrosis (Chen et al., 2021). Glaucoma TM tissue has excess ECM so we investigated CDH11 protein levels in normal and glaucomatous TM cells. Western immunoblots and densitometry showed that CDH11 protein levels were significantly increased in GTM cells compared to NTM cells (Figure 4A,B). However, there was no significant difference in mDia2 or Eps8 protein levels between NTM and GTM cells (Figure 4B). We then investigated the effects of 24 h mechanical stretch. There was no difference in CDH11, mDia2, or Eps8 protein levels when comparing stretched vs. non-stretched cells (Figure 4C). Thus, CDH11 is upregulated in glaucoma TM cells, but mechanical stretch does not appear to additionally affect expression levels.

We also investigated whether mechanical stretch affected Myo10 protein levels. Consistent with our previous observations (Sun et al., 2019a), Myo10 levels were not significantly different between non-stretched NTM and GTM cells. However, in response to mechanical stretch, Myo10 protein levels in GTM cells showed a small (~5%), but significant increase after 24 h compared to NTM cells by Western immunoblot and densitometry (Figure 4D). Over-expression of Myo10 has been shown to induce TNTs (Gousset et al., 2013). Therefore, we hypothesized that increased Myo10 protein levels in mechanically stretched GTM cells may affect cellular communication via TNTs so we performed a fluorescent vesicle transfer assay. In non-stretched cells, GTM cells showed significantly more vesicle transfer compared to NTM cells (Figure 4E), as we found previously (Sun et al., 2019a). Yet, 24 h mechanical stretch did not significantly affect vesicle transfer in NTM cells or GTM cells.

## DISCUSSION

In this study, we show that mechanical stretch, a proxy for elevated IOP, affects the composition and distribution of proteins in TM cell filopodia and vesicle transfer in TNTs. Specifically, we show that TM filopodia contain Myo10, integrins  $\alpha 5 \beta 1$  and  $\alpha v \beta 3$ , and to some extent  $\alpha v \beta 5$  integrin, and CDH11, Eps8, and mDia2. Mechanical stretch specifically activated  $\beta 1$  integrin within 1 h, as shown with conformation-specific monoclonal antibodies, suggesting that certain integrins become activated as a rapid response to the stretch and distortion caused by elevated IOP. In addition, mechanical stretch increased the number of CDH11-negative TM cells suggesting that other cell surface adhesion molecules are also affected. In contrast, mechanical stretch had no effect on vesicle transfer via TNTs in either NTM or GTM. Together, these data suggest that filopodial-associated and cell-surface proteins are dynamically altered in response to their biomechanical environment, but these mechanical cues do not significantly impact cellular communication via TNTs. In addition, it provides additional

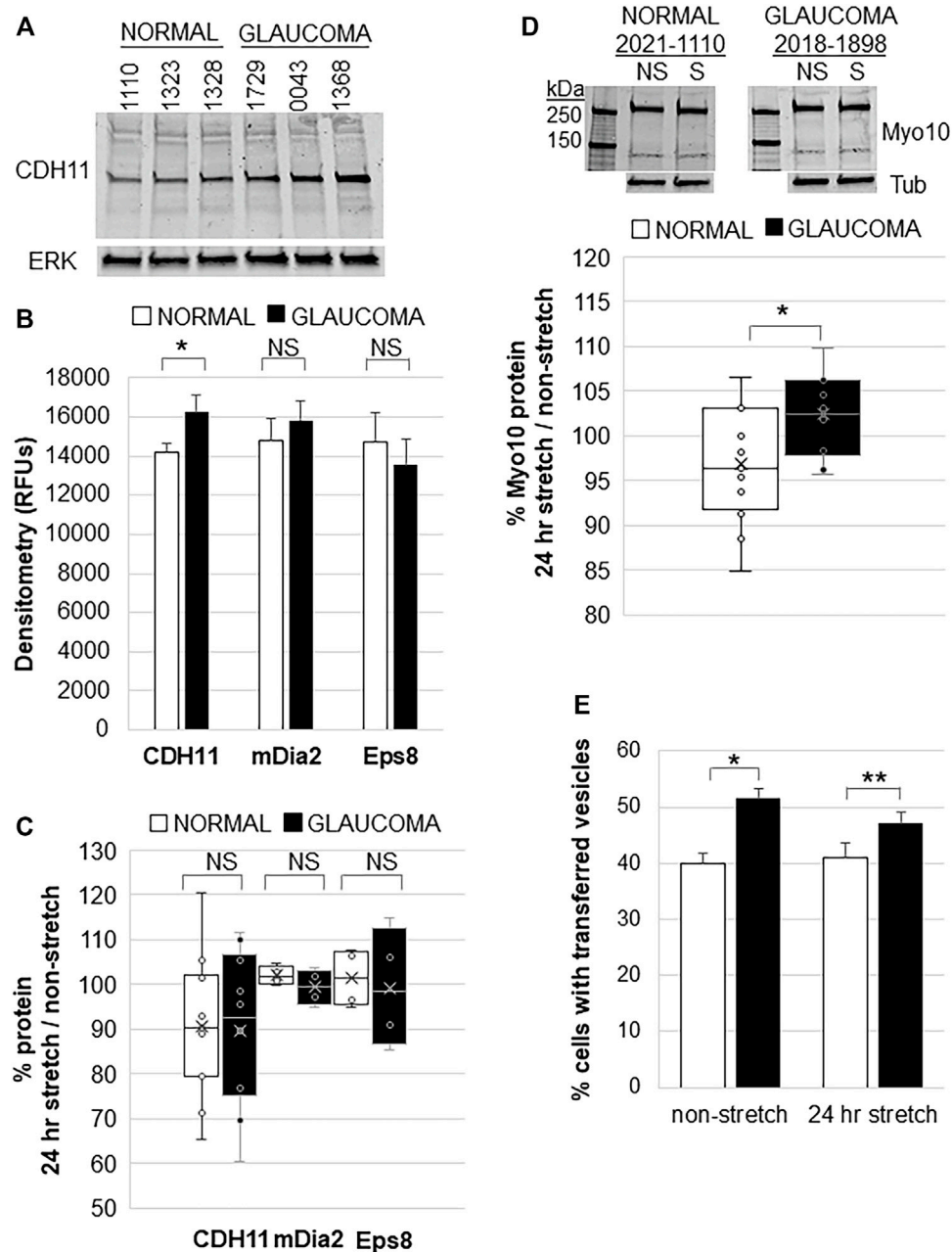


**FIGURE 4** | Filopodial proteins in normal and glaucomatous TM cells in response to 24 h mechanical stretch. **(A)** CDH11 protein levels in normal and glaucoma TM cell lysates. ERK1 was used as a loading control. **(B)** Densitometry of CDH11, mDia2, and Eps8 protein levels showed significantly increased levels in glaucoma TM cells. Relative fluorescent units (RFUs) were normalized for ERK loading. Normal:  $n = 17$  replicates from 15 NTM cell strains; Glaucoma:  $n = 16$  technical replicates from 10 GTM cell strains. \* $p = 0.038$  by ANOVA; NS = not significant. **(C)** Densitometry of CDH11 protein by Western immunoblotting of normal and glaucomatous TM cells after 24 h mechanical stretch. Data show stretch/non-stretched as a percentage. NS = not significant. Normal:  $n = 11$  replicates from 10 NTM cell strains; Glaucoma:  $n = 10$  technical replicates from 7 GTM cell strains. **(D)** Representative Western immunoblot of Myo10 protein in NTM and GTM cells with and without 24 h mechanical stretch. Tubulin (tub) was used as a loading control. Densitometry showed that GTM cells had a small (~5%), but significantly increased level of Myo10 protein after 24 h mechanical stretch. \* $p = 0.023$  by ANOVA. Normal:  $n = 15$  replicates from 7 NTM cell strains; Glaucoma:  $n = 10$  technical replicates from 5 GTM cell strains. **(E)** TM cells were labeled separately with DiO or DiD dyes, mixed and then mechanically stretched for 24 h. The number of cells containing fluorescent vesicles of the opposite color were counted for normal or glaucomatous cells, with and without stretch. Glaucoma TM cells had significantly increased transfer of vesicles compared to normal TM cells, but mechanical stretch did not cause a significant change. Data show mean  $\pm$  s.e.m. \* $p = 0.001$ ; \*\* $p = 0.015$  by ANOVA.



evidence that the function of TNTs and filopodia are different, as previously suggested (Ljubojevic et al., 2021).

Since only heterodimer integrins, not individual subunits, are expressed on the cell surface, and the  $\alpha 5$  subunit only pairs with the  $\beta 1$  subunit, localization of the  $\alpha 5$  subunit must indicate the presence of the  $\alpha 5\beta 1$  integrin heterodimer in filopodia (Hynes, 2002). Localization of  $\alpha 5\beta 1$  integrin at the filopodial tip suggests that it is actively engaged with the underlying substrate in a nascent adhesion.  $\alpha 5\beta 1$  integrin binding to fibronectin could initiate fibronectin fibrillogenesis or focal adhesion formation in the immediate area, further stabilizing the filopodia (Singh et al., 2010). The discrete areas of  $\alpha 5\beta 1$  integrin along the shaft may indicate nascent adhesions (Henning Stumpf et al., 2020). This agrees with the 2-step theory of filopodial elongation, where integrins transiently engage the substrate to stabilize it while additional components are transported toward the tip by Myo10 (He et al., 2017).

Using conformation-specific antibodies (Byron et al., 2009), we showed that mechanical stretch activated  $\beta 1$  integrin, but not  $\alpha 5$  or  $\alpha \nu \beta 3$  integrins. This suggests that  $\alpha 5\beta 1$  integrin may not be involved in detecting mechanical stretch.  $\beta 1$  integrin heterodimerizes with several other  $\alpha$  subunits expressed in the TM (Filla et al., 2017). One possibility is  $\alpha 4\beta 1$  integrin, which cross-talks with  $\alpha 1\beta 1$  and  $\alpha 2\beta 1$  integrins (Schwinn et al., 2010; Faralli et al., 2011), and is recognized by the Huts-21 antibody (Njus et al., 2009). Other possibilities are the collagen binding  $\alpha 1\beta 1$  or  $\alpha 2\beta 1$  integrins (Luque et al., 1996). Further studies are required to reveal the exact identity of integrin heterodimers involved in sensing mechanical stretch-induced alterations to the biomechanical environment.

In this study, we show that Myo10 may play a role in transporting  $\alpha 5\beta 1$  integrins to the filopodial tip, as suggested in several cell types (Zhang et al., 2004; He et al., 2017; Miihkinen et al., 2021). The distribution and colocalization of Myo10 with  $\alpha 5$  and  $\beta 1$  integrins in filopodia of TM cells supports this idea. However, our pull-down data provide further nuances to Myo10- $\alpha 5\beta 1$  integrin interactions. Myo10 showed positive interaction with the  $\alpha 5$  integrin subunit, but not with  $\beta 1$  integrin. This suggests that Myo10 must be interacting with the  $\alpha 5\beta 1$  integrin heterodimer via the  $\alpha 5$  integrin subunit. An earlier study supports this possibility and found  $\alpha 5$  integrin can interact with Myo10 in U2-OS osteosarcoma cells (Miihkinen et al., 2021). Our pull-down assays used the SNAKA51 conformation-specific antibody, thereby showing a positive interaction of Myo10 and activated  $\alpha 5$  integrin. Had we used a pan  $\alpha 5$ -integrin antibody, it is possible that no interaction would have been detected. Nevertheless, our data suggest that different cell types may use either the  $\alpha 5$  or the  $\beta 1$  integrin subunit when binding Myo10 (Zhang et al., 2004; Miihkinen et al., 2021).

The pull-down assays also showed positive interactions of Myo10 with  $\alpha \nu \beta 3$  and  $\alpha \nu \beta 5$  integrins. These data expand the repertoire of integrins that bind to Myo10.  $\alpha \nu \beta 3$  integrin is involved in phagocytosis, TGF $\beta$  signaling, and is activated by dexamethasone in TM cells (Filla et al., 2011; Faralli et al., 2019; Filla et al., 2021). In addition,  $\alpha \nu \beta 3$  integrin activation caused a significant IOP increase in mice (Faralli et al., 2019). Our immunostaining data suggest that Myo10 may traffic  $\alpha \nu \beta 3$

integrin to the filopodia tip, like its role for  $\beta 1$  integrin. Also,  $\alpha \nu \beta 3$  integrin may be involved in transiently binding to ECM substrates in nascent adhesions in the filopodial shaft and tip (Henning Stumpf et al., 2020). Our prior live imaging studies showed that filopodial tips are cleaved, which allows the filopodia to retract back toward the cell (Keller and Kopczynski, 2020). The cleaved filopodial tips were immunolabeled with several ECM proteins, including  $\alpha \nu \beta 5$  integrin. This is consistent with the lack of  $\alpha \nu \beta 5$  integrin immunostaining in filopodia shown in this study. It also suggests that Myo10- $\alpha \nu \beta 5$  integrin interactions are important for other TM cell functions.

CDH11 was found associated with filopodia/TNTs connecting TM cells. However, CDH11 immunostaining was not specifically localized to nascent adhesions of the filopodia shaft or tips, but instead, CDH11 was detected along the entire length of the filopodia. Recently, CDH11 was found to localize to focal adhesions, where it binds fibronectin via an interaction with syndecan-4 (Langhe et al., 2016). CDH11 is linked to fibrotic diseases such as liver fibrosis, scleroderma, and pulmonary fibrosis (Chen et al., 2021), and CDH11 is up-regulated by TGF $\beta 2$  (Wecker et al., 2013). Therefore, the increased CDH11 protein levels in glaucomatous TM cells is perhaps not surprising. However, we cannot rule out that CDH11 levels may be influenced by prior medications that glaucomatous eyes were subject to. CDH11 forms adhesion complexes, which are dynamically turned over. Here, we show that 1-h of mechanical stretch reduced cell surface CDH11. This could indicate that mechanical stretch induces internalization by TM cells, possibly via clathrin-mediated endocytosis, which is utilized by prostate cancer cells (Satcher et al., 2015). Alternatively, mechanical stretch may induce cleavage of the CDH11 extracellular domain, where the epitope is located. Mechanical stretch and elevated IOP initiates activation of various proteases, including ADAMs and ADAMTSs (Vittitow and Borrás, 2004; Vittal et al., 2005). In neural crest cells, ADAMs cleave CDH11 (McCusker et al., 2009), so it is possible that these proteases may cleave CDH11 to reduce the extracellular epitope on the cell surface of mechanically stretched TM cells. Whichever mechanism is utilized, our mechanical stretch data suggest that reduced CDH11 could disrupt cell-cell adhesions and cell-ECM adhesions in TM tissue at elevated IOP.

Myo10 protein levels had small, but significant increases in mechanically stretched GTM cells. During normal filopodia dynamics, Myo10 travels towards the tip of the filopodia during actin assembly and growth, and displays rearward movement as the filopodia is retracted to the cell (Berg and Cheney, 2002). Because actin dynamics are impaired in glaucoma TM cells (Sun et al., 2019a; Keller and Kopczynski, 2020), Myo10 may be expressed longer on glaucomatous filopodia. This may explain increased Myo10 protein levels in mechanically stretch glaucoma cells. However, the lysates were harvested from whole cells, rather than from filopodia specifically. Myo10 also localizes to podosome or invadopodia-like structures (PILS) and PILS are increased by mechanical stretch (Aga et al., 2008;

McMichael et al., 2010; Sun et al., 2019b). Thus, the observed increase in Myo10 protein may additionally reflect increased Myo10 at PILS.

In summary, we have shown that Myo10 binds to a wider range of integrins than previously reported. In addition, mechanical stretch specifically and rapidly activates  $\beta 1$  integrin, while reducing CDH11 on TM cell surface. These data provide novel information regarding the cellular structures and transmembrane adhesive proteins that TM cells use to sense changes to the biomechanical environment such as those changes caused by elevated IOP.

## DATA AVAILABILITY STATEMENT

The original contributions presented in the study are included in the article/**Supplementary Material**, further inquiries can be directed to the corresponding author.

## ETHICS STATEMENT

Ethical review and approval was not required for the study on human participants in accordance with the local legislation and institutional requirements. Written informed consent from the next of kin was not required to participate in this study in accordance with the national legislation and the institutional requirements.

## REFERENCES

- Aboutis, S., Delage, E., and Zurzolo, C. (2015). Identification and Characterization of Tunneling Nanotubes for Intercellular Trafficking. *Curr. Protoc. Cel Biol* 67, 12–21. doi:10.1002/0471143030.cb1210s67
- Acott, T. S., and Kelley, M. J. (2008). Extracellular Matrix in the Trabecular Meshwork. *Exp. Eye Res.* 86, 543–561. doi:10.1016/j.exer.2008.01.013
- Acott, T. S., Vranka, J. A., Keller, K. E., Raghunathan, V., and Kelley, M. J. (2021). Normal and Glaucomatous Outflow Regulation. *Prog. Retin. Eye Res.* 82, 100897. doi:10.1016/j.preteyeres.2020.100897
- Aga, M., Bradley, J. M., Keller, K. E., Kelley, M. J., and Acott, T. S. (2008). Specialized Podosome- or Invadopodia-like Structures (PILS) for Focal Trabecular Meshwork Extracellular Matrix Turnover. *Invest. Ophthalmol. Vis. Sci.* 49, 5353–5365. doi:10.1167/iops.07-1666
- Almagro, S., Durmort, C., Chervin-Pe'tinot, A., Heyraud, S., Dubois, M., Lambert, O., et al. (2010). The Motor Protein Myosin-X Transports VE-Cadherin along Filopodia to Allow the Formation of Early Endothelial Cell-Cell Contacts. *Mol. Cel Biol* 30, 1703–1717. doi:10.1128/mcb.01226-09
- Berg, J. S., and Cheney, R. E. (2002). Myosin-X Is an Unconventional Myosin that Undergoes Intrafilopodial Motility. *Nat. Cel Biol* 4, 246–250. doi:10.1038/ncb762
- Bohil, A. B., Robertson, B. W., and Cheney, R. E. (2006). Myosin-X Is a Molecular Motor that Functions in Filopodia Formation. *Proc. Natl. Acad. Sci. U.S.A.* 103, 12411–12416. doi:10.1073/pnas.0602443103
- Bradley, J. M., Kelley, M. J., Zhu, X., Anderssohn, A. M., Alexander, J. P., and Acott, T. S. (2001). Effects of Mechanical Stretching on Trabecular Matrix Metalloproteinases. *Invest. Ophthalmol. Vis. Sci.* 42, 1505–1513.
- Byron, A., Humphries, J. D., Askari, J. A., Craig, S. E., Mould, A. P., and Humphries, M. J. (2009). Anti-integrin Monoclonal Antibodies. *J. Cell Sci* 122, 4009–4011. doi:10.1242/jcs.056770
- Chen, X., Xiang, H., Yu, S., Lu, Y., and Wu, T. (2021). Research Progress in the Role and Mechanism of Cadherin-11 in Different Diseases. *J. Cancer* 12, 1190–1199. doi:10.7150/jca.52720

## AUTHOR CONTRIBUTIONS

Conceptualization: KK; performed experiments: Y-FY, YS, and KK; data analysis: Y-FY, DP, and KK; writing: KK; editing: Y-FY, DP, and KK; funding acquisition: DP, KK.

## FUNDING

NIH/NEI R01 EY019643 (KK), P30 EY010572 (KK), R01 EY017006 (DP), P30 EY016665 (DP) and unrestricted grant to the Casey Eye Institute from Research to Prevent Blindness, NY.

## ACKNOWLEDGMENTS

The authors would like to thank Lions VisionGift, Portland, OR for procurement of normal and glaucoma cadaver eyes from which the TM cells were derived.

## SUPPLEMENTARY MATERIAL

The Supplementary Material for this article can be found online at: <https://www.frontiersin.org/articles/10.3389/fcell.2022.886706/full#supplementary-material>

- Clark, K., Pankov, R., Travis, M. A., Askari, J. A., Mould, A. P., Craig, S. E., et al. (2005). A Specific  $\alpha 5\beta 1$ -integrin Conformation Promotes Directional Integrin Translocation and Fibronectin Matrix Formation. *J. Cell Sci* 118, 291–300. doi:10.1242/jcs.01623
- Du, X., Gu, M., Weisel, J. W., Nagaswami, C., Bennett, J. S., Bowditch, R., et al. (1993). Long Range Propagation of Conformational Changes in Integrin Alpha IIB Beta 3. *J. Biol. Chem.* 268, 23087–23092. doi:10.1016/s0021-9258(19)49429-5
- Faralli, J. A., Filla, M. S., and Peters, D. M. (2019). Effect of  $\alpha \beta 3$  Integrin Expression and Activity on Intraocular Pressure. *Invest. Ophthalmol. Vis. Sci.* 60, 1776–1788. doi:10.1167/iops.18-26038
- Faralli, J. A., Newman, J. R., Sheibani, N., Dedhar, S., and Peters, D. M. (2011). Integrin-linked Kinase Regulates Integrin Signaling in Human Trabecular Meshwork Cells. *Invest. Ophthalmol. Vis. Sci.* 52, 1684–1692. doi:10.1167/iops.10-6397
- Fierro-González, J. C., White, M. D., Silva, J. C., and Plachta, N. (2013). Cadherin-dependent Filopodia Control Preimplantation Embryo Compaction. *Nat. Cel Biol* 15, 1424–1433. doi:10.1038/ncb2875
- Filla, M. S., Faralli, J. A., Peotter, J. L., and Peters, D. M. (2017). The Role of Integrins in Glaucoma. *Exp. Eye Res.* 158, 124–136. doi:10.1016/j.exer.2016.05.011
- Filla, M. S., Meyer, K. K., Faralli, J. A., and Peters, D. M. (2021). Overexpression and Activation of  $\alpha \beta 3$  Integrin Differentially Affects TGF $\beta 2$  Signaling in Human Trabecular Meshwork Cells. *Cells* 10. doi:10.3390/cells10081923
- Filla, M. S., Schwinn, M. K., Nosie, A. K., Clark, R. W., and Peters, D. M. (2011). Dexamethasone-Associated Cross-Linked Actin Network Formation in Human Trabecular Meshwork Cells Involves  $\beta 3$  Integrin Signaling. *Invest. Ophthalmol. Vis. Sci.* 52, 2952–2959. doi:10.1167/iops.10-6618
- Fuchshofer, R., and Tamm, E. R. (2009). Modulation of Extracellular Matrix Turnover in the Trabecular Meshwork. *Exp. Eye Res.* 88, 683–688. doi:10.1016/j.exer.2009.01.005
- Gagen, D., Faralli, J. A., Filla, M. S., and Peters, D. M. (2014). The Role of Integrins in the Trabecular Meshwork. *J. Ocul. Pharmacol. Ther.* 30, 110–120. doi:10.1089/jop.2013.0176

- Gousset, K., Marzo, L., Commere, P.-H., and Zurzolo, C. (2013). Myo10 Is a Key Regulator of TNT Formation in Neuronal Cells. *J. Cell Sci* 126, 4424–4435. doi:10.1242/jcs.129239
- Grierson, I., and Lee, W. R. (1977). Light Microscopic Quantitation of the Endothelial Vacuoles in Schlemm's Canal. *Am. J. Ophthalmol.* 84, 234–246. doi:10.1016/0002-9394(77)90857-1
- He, K., Sakai, T., Tsukasaki, Y., Watanabe, T. M., and Ikebe, M. (2017). Myosin X Is Recruited to Nascent Focal Adhesions at the Leading Edge and Induces Multi-Cycle Filopodial Elongation. *Sci. Rep.* 7, 13685. doi:10.1038/s41598-017-06147-6
- Henning Stumpf, B., Ambriović-Ristov, A., Radenovic, A., and Smith, A.-S. (2020). Recent Advances and Prospects in the Research of Nascent Adhesions. *Front. Physiol.* 11, 574371. doi:10.3389/fphys.2020.574371
- Hynes, R. O. (2002). Integrins. *Cell* 110, 673–687. doi:10.1016/s0092-8674(02)00971-6
- Katsumi, A., Naoe, T., Matsushita, T., Kaibuchi, K., and Schwartz, M. A. (2005). Integrin Activation and Matrix Binding Mediate Cellular Responses to Mechanical Stretch. *J. Biol. Chem.* 280, 16546–16549. doi:10.1074/jbc.c400455200
- Keller, K. E., and Kopczynski, C. (2020). Effects of Netarsudil on Actin-Driven Cellular Functions in Normal and Glaucomatous Trabecular Meshwork Cells: A Live Imaging Study. *J. Clin. Med.* 9, 3524. doi:10.3390/jcm9113524
- Keller, K. E., Bhattacharya, S. K., Borrás, T., Brunner, T. M., Chansangpetch, S., Clark, A. F., et al. (2018). Consensus Recommendations for Trabecular Meshwork Cell Isolation, Characterization and Culture. *Exp. Eye Res.* 171, 164–173. doi:10.1016/j.exer.2018.03.001
- Keller, K. E., Bradley, J. M., Sun, Y. Y., Yang, Y.-F., and Acott, T. S. (2017). Tunneling Nanotubes Are Novel Cellular Structures that Communicate Signals between Trabecular Meshwork Cells. *Invest. Ophthalmol. Vis. Sci.* 58, 5298–5307. doi:10.1167/iovs.17-22732
- Keller, K. E., and Peters, D. M. (2022). Pathogenesis of Glaucoma: Extracellular Matrix Dysfunction in the Trabecular Meshwork-A Review. *Clin. Exp. Ophthalmol.* 50, 163–182. doi:10.1111/ceo.14027
- Lai, M., Guo, Y., Ma, J., Yu, H., Zhao, D., Fan, W., et al. (2015). Myosin X Regulates Neuronal Radial Migration through Interacting with N-Cadherin. *Front. Cell Neurosci.* 9, 326. doi:10.3389/fncel.2015.00326
- Langhe, R. P., Gudzenko, T., Bachmann, M., Becker, S. F., Gonnermann, C., Winter, C., et al. (2016). Cadherin-11 Localizes to Focal Adhesions and Promotes Cell-Substrate Adhesion. *Nat. Commun.* 7, 10909. doi:10.1038/ncomms10909
- Last, J. A., Pan, T., Ding, Y., Reilly, C. M., Keller, K., Acott, T. S., et al. (2011). Elastic Modulus Determination of normal and Glaucomatous Human Trabecular Meshwork. *Invest. Ophthalmol. Vis. Sci.* 52, 2147–2152. doi:10.1167/iovs.10-6342
- Ljubojevic, N., Henderson, J. M., and Zurzolo, C. (2021). The Ways of Actin: Why Tunneling Nanotubes Are Unique Cell Protrusions. *Trends Cell Biol.* 31, 130–142. doi:10.1016/j.tcb.2020.11.008
- Luque, A., Gómez, M., Puzon, W., Takada, Y., Sánchez-Madrid, F., and Cabañas, C. (1996). Activated Conformations of Very Late Activation Integrins Detected by a Group of Antibodies (HUTS) Specific for a Novel Regulatory Region(355-425) of the Common  $\beta$ 1 Chain. *J. Biol. Chem.* 271, 11067–11075. doi:10.1074/jbc.271.19.11067
- Mattila, P. K., and Lappalainen, P. (2008). Filopodia: Molecular Architecture and Cellular Functions. *Nat. Rev. Mol. Cell Biol* 9, 446–454. doi:10.1038/nrm2406
- Mccusker, C., Cousin, H., Neuner, R., and Alfandari, D. (2009). Extracellular Cleavage of Cadherin-11 by ADAM Metalloproteases Is Essential forXenopusCranial Neural Crest Cell Migration. *MBoC* 20, 78–89. doi:10.1091/mbc.e08-05-0535
- Mcmichael, B. K., Cheney, R. E., and Lee, B. S. (2010). Myosin X Regulates Sealing Zone Patterning in Osteoclasts through Linkage of Podosomes and Microtubules. *J. Biol. Chem.* 285, 9506–9515. doi:10.1074/jbc.m109.017269
- Miihkinen, M., Grönloh, M. L. B., Popović, A., Vihinen, H., Jokitalo, E., Goult, B. T., et al. (2021). Myosin-X and Talin Modulate Integrin Activity at Filopodia Tips. *Cell Rep.* 36, 109716. doi:10.1016/j.celrep.2021.109716
- Njus, B. H., Chigaev, A., Waller, A., Wlodek, D., Ostopovici-Halip, L., Ursu, O., et al. (2009). Conformational mAb as a Tool for Integrin Ligand Discovery. *ASSAY Drug Develop. Tech.* 7, 507–515. doi:10.1089/adt.2009.0203
- Raghunathan, V., Benoit, J., Kasetti, R., Zode, G., Salemi, M., Phinney, B. S., et al. (2018). Glaucomatous Cell Derived Matrices Differentially Modulate Non-glaucomatous Trabecular Meshwork Cellular Behavior. *Acta Biomater.* doi:10.1016/j.actbio.2018.02.037
- Rustom, A., Saffrich, R., Markovic, I., Walther, P., and Gerdes, H.-H. (2004). Nanotubular Highways for Intercellular Organelle Transport. *Science* 303, 1007–1010. doi:10.1126/science.1093133
- Satcher, R. L., Pan, T., Bilén, M. A., Li, X., Lee, Y. C., Ortiz, A., et al. (2015). Cadherin-11 Endocytosis Through Binding to Clathrin Promotes Cadherin-11-Mediated Migration in Prostate Cancer Cells. *J. Cell Sci* 128, 4629–4641. doi:10.1242/jcs.176081
- Schwinn, M. K., Gonzalez, J. M., Jr., Gabelt, B. A. T., Sheibani, N., Kaufman, P. L., and Peters, D. M. (2010). Heparin II Domain of Fibronectin Mediates Contractility through an  $\alpha$ 4 $\beta$ 1 Co-signaling Pathway. *Exp. Cell Res.* 316, 1500–1512. doi:10.1016/j.yexcr.2010.03.010
- Singh, P., Carraher, C., and Schwarzbauer, J. E. (2010). Assembly of Fibronectin Extracellular Matrix. *Annu. Rev. Cell Dev. Biol.* 26, 397–419. doi:10.1146/annurev-cellbio-100109-104020
- Stamer, W. D., and Acott, T. S. (2012). Current Understanding of Conventional Outflow Dysfunction in Glaucoma. *Curr. Opin. Ophthalmol.* 23, 135–143. doi:10.1097/icu.0b013e32834ff23e
- Sun, Y. Y., Bradley, J. M., and Keller, K. E. (2019a). Phenotypic and Functional Alterations in Tunneling Nanotubes Formed by Glaucomatous Trabecular Meshwork Cells. *Invest. Ophthalmol. Vis. Sci.* 60, 4583–4595. doi:10.1167/iovs.19-28084
- Sun, Y. Y., Yang, Y.-F., and Keller, K. E. (2019b). Myosin-X Silencing in the Trabecular Meshwork Suggests a Role for Tunneling Nanotubes in Outflow Regulation. *Invest. Ophthalmol. Vis. Sci.* 60, 843–851. doi:10.1167/iovs.18-26055
- Tektas, O.-Y., and Lütjen-Drecoll, E. (2009). Structural Changes of the Trabecular Meshwork in Different Kinds of Glaucoma. *Exp. Eye Res.* 88, 769–775. doi:10.1016/j.exer.2008.11.025
- Tham, Y.-C., Li, X., Wong, T. Y., Quigley, H. A., Aung, T., and Cheng, C.-Y. (2014). Global Prevalence of Glaucoma and Projections of Glaucoma Burden through 2040. *Ophthalmology* 121, 2081–2090. doi:10.1016/j.ophtha.2014.05.013
- Tzima, E., Del Pozo, M. A., Shattil, S. J., Chien, S., and Schwartz, M. A. (2001). Activation of Integrins in Endothelial Cells by Fluid Shear Stress Mediates Rho-dependent Cytoskeletal Alignment. *EMBO J.* 20, 4639–4647. doi:10.1093/emboj/20.17.4639
- Vittal, V., Rose, A., Gregory, K. E., Kelley, M. J., and Acott, T. S. (2005). Changes in Gene Expression by Trabecular Meshwork Cells in Response to Mechanical Stretching. *Invest. Ophthalmol. Vis. Sci.* 46, 2857–2868. doi:10.1167/iovs.05-0075
- Vittitow, J., and Borrás, T. (2004). Genes Expressed in the Human Trabecular Meshwork during Pressure-Induced Homeostatic Response. *J. Cell Physiol.* 201, 126–137. doi:10.1002/jcp.20030
- Vranka, J. A., Kelley, M. J., Acott, T. S., and Keller, K. E. (2015). Extracellular Matrix in the Trabecular Meshwork: Intraocular Pressure Regulation and Dysregulation in Glaucoma. *Exp. Eye Res.* 133, 112–125. doi:10.1016/j.exer.2014.07.014

- Watanabe, T. M., Tokuo, H., Gonda, K., Higuchi, H., and Ikebe, M. (2010). Myosin-X Induces Filopodia by Multiple Elongation Mechanism. *J. Biol. Chem.* 285, 19605–19614. doi:10.1074/jbc.m109.093864
- Webber, H. C., Bermudez, J. Y., Millar, J. C., Mao, W., and Clark, A. F. (2018). The Role of Wnt/ $\beta$ -Catenin Signaling and K-Cadherin in the Regulation of Intraocular Pressure. *Invest. Ophthalmol. Vis. Sci.* 59, 1454–1466. doi:10.1167/iovs.17-21964
- Wecker, T., Han, H., Börner, J., Grehn, F., and Schlunck, G. (2013). Effects of TGF- $\beta$ 2 on Cadherins and  $\beta$ -Catenin in Human Trabecular Meshwork Cells. *Invest. Ophthalmol. Vis. Sci.* 54, 6456–6462. doi:10.1167/iovs.13-12669
- Wirtz, M. K., Sykes, R., Samples, J., Edmunds, B., Choi, D., Keene, D. R., et al. (2021). Identification of Missense Extracellular Matrix Gene Variants in a Large Glaucoma Pedigree and Investigation of the N700S Thrombospondin-1 Variant in Normal and Glaucomatous Trabecular Meshwork Cells. *Curr. Eye Res.*, 1–12. doi:10.1080/02713683.2021.1945109
- Zhang, H., Berg, J. S., Li, Z., Wang, Y., Lång, P., Sousa, A. D., et al. (2004). Myosin-X Provides a Motor-Based Link between Integrins and the Cytoskeleton. *Nat. Cell Biol.* 6, 523–531. doi:10.1038/ncb1136

**Conflict of Interest:** The authors declare that the research was conducted in the absence of any commercial or financial relationships that could be construed as a potential conflict of interest.

**Publisher's Note:** All claims expressed in this article are solely those of the authors and do not necessarily represent those of their affiliated organizations, or those of the publisher, the editors and the reviewers. Any product that may be evaluated in this article, or claim that may be made by its manufacturer, is not guaranteed or endorsed by the publisher.

Copyright © 2022 Yang, Sun, Peters and Keller. This is an open-access article distributed under the terms of the Creative Commons Attribution License (CC BY). The use, distribution or reproduction in other forums is permitted, provided the original author(s) and the copyright owner(s) are credited and that the original publication in this journal is cited, in accordance with accepted academic practice. No use, distribution or reproduction is permitted which does not comply with these terms.